Environmental Science & Technology

Article

Cite This: Environ. Sci. Technol. 2019, 53, 3718−3728

pubs.acs.org/est

Defluorination of Per- and Polyfluoroalkyl Substances (PFASs) with Hydrated Electrons: Structural Dependence and Implications to PFAS Remediation and Management

Michael J. Bentel,[†] Yaochun Yu,[§] Lihua Xu,[†] Zhong Li,[∥] Bryan M. Wong,[†,‡] Yujie Men,[§,⊥] and Jinyong Liu*[,†]

[†]Department of Chemical & Environmental Engineering and [‡]Materials Science & Engineering Program, University of California, Riverside, California 92521, United States

[§]Department of Civil & Environmental Engineering, [∥]Metabolomics Lab of Roy J. Carver Biotechnology Center, and [⊥]Institute for Genomic Biology, University of Illinois at Urbana−Champaign, Urbana, Illinois 61801, United States

Supporting Information

ABSTRACT: This study investigates critical structure−reactivity relationships within 34 representative per- and polyfluoroalkyl substances (PFASs) undergoing defluorination with UV-generated hydrated electrons. While C_nF_{2n+1}−COO^- with variable fluoroalkyl chain lengths (n = 2 to 10) exhibited a similar rate and extent of parent compound decay and defluorination, the reactions of telomeric C_nF_{2n+1}−CH_2CH_2−COO^- and C_nF_{2n+1}−SO_3^- showed an apparent dependence on the length of the fluoroalkyl chain. Cross comparison of experimental results, including different rates of decay and defluorination of specific PFAS categories, the incomplete defluorination from most PFAS structures, and the surprising 100% defluorination from CF_3COO^-, leads to the elucidation of new mechanistic insights into PFAS degradation. Theoretical calculations on the C−F bond dissociation energies (BDEs) of all PFAS structures reveal strong relationships among (i) the rate and extent of decay and defluorination, (ii) head functional groups, (iii) fluoroalkyl chain length, and (iv) the position and number of C−F bonds with low BDEs. These relationships are further supported by the spontaneous cleavage of specific bonds during calculated geometry optimization of PFAS structures bearing one extra electron, and by the product analyses with high-resolution mass spectrometry. Multiple reaction pathways, including H/F exchange, dissociation of terminal functional groups, and decarboxylation-triggered HF elimination and hydrolysis, result in the formation of variable defluorination products. The selectivity and ease of C−F bond cleavage highly depends on molecular structures. These findings provide critical information for developing PFAS treatment processes and technologies to destruct a wide scope of PFAS pollutants and for designing fluorochemical formulations to avoid releasing recalcitrant PFASs into the environment.

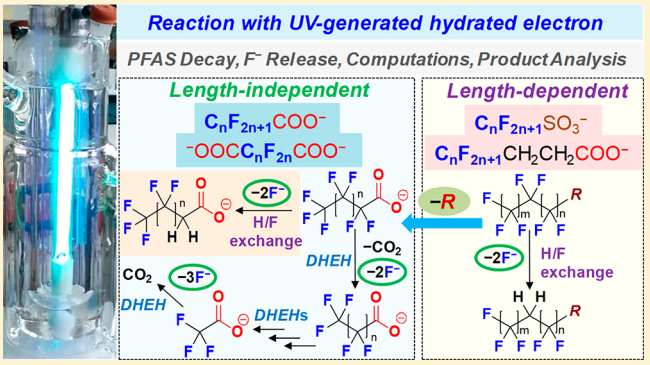

INTRODUCTION

The manufacturing, application, and disposal of fluorochemicals since the 1940s have led to worldwide pollution by per- and polyfluoroalkyl substances (PFASs).[1,2] The U.S. EPA listed C7, C8, and C9 perfluorinated carboxylic acids (PFCAs) and C4, C6, and C8 perfluorinated sulfonic acids (PFSAs) on the Third Unregulated Contaminant Monitoring Rule (UCMR 3) in 2012,[3] and established health advisory levels for C8 perfluorooctanoic acid (PFOA) and perfluorooctanesulfonic acid (PFOS) in drinking water in 2016.[4] Very recently, the states of Vermont[5] and Massachusetts[6] have updated the health advisory for five of the six PFASs in the UCMR 3 list (except for the C4 perfluorobutanesulfonic acid PFBS). The state of New Jersey adopted the maximum contaminant level of C9 perfluorononanoic acid (PFNA),[7] and the state of North Carolina established the health advisory level for perfluoro-2-propoxypropanoic acid (GenX).[8] Regulation has triggered substantial interest and efforts in developing PFAS treatment technologies.[9,10] While physical separation (e.g., carbon adsorption, membrane filtration, and ion exchange) enables rapid PFAS removal from water,[11−13] the enriched PFASs in physical separation wastes must be destroyed. Groundwater remediation and the treatment of PFASs in obsolete products and industrial wastes also require cost-effective destruction methods. Due to the challenges in cleaving highly stable C−F bonds (i.e., defluorination),[10] novel technologies such as electrochemical,[14−17] sonochemical,[18−20] photocatalytic,[21−23]

Received: November 25, 2018
Revised: February 16, 2019
Accepted: March 2, 2019
Published: March 15, 2019

DOI: 10.1021/acs.est.8b06648
Environ. Sci. Technol. 2019, 53, 3718−3728

mechanochemical,[24,25] plasmatic,[26] radiolytic,[27] and other oxidative and reductive methods[9,28] have been developed for the defluorination of C8 PFOA and/or PFOS.

However, PFASs have often been applied in complicated mixtures. For example, aqueous film-forming foams (AFFF) for fire-fighting contain at least hundreds of PFAS structures,[29−31] most of which contain a fluorocarbon moiety with variable lengths and head groups connecting to highly diverse organic moieties (Figure 1). A large diversity of PFAS

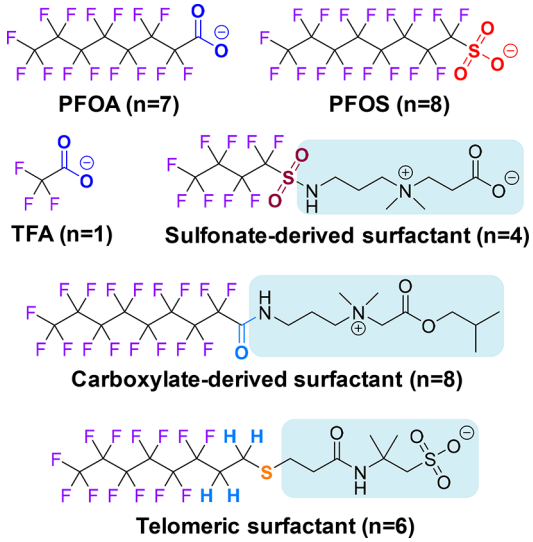

Figure 1. Examples of PFAS structures detected in the environment (n indicating the variable length of C_nF_{2n+1} shown in the figure; organic moiety in AFFF surfactants shaded in blue). Surfactant structures were taken from refs 29 and 31.

structures has been identified in water bodies polluted by fluorochemical industries,[32−35] fire-fighting practices,[29,30,36] and landfill leachates.[37] The extending list of regulated PFASs calls for the investigation into the treatment of PFASs beyond PFOA and PFOS. A fundamental and critical question is thus raised regarding the remediation of PFAS pollution: would the technologies developed for PFOA/PFOS defluorination remain effective for other PFAS structures? Alternatively, what structural factors control the rate and extent of PFAS defluorination?

Studies on the chemical destruction of other PFASs beyond PFOA/PFOS (e.g., shorter chain analogues or new structures) have been very limited. While a small number of studies has tested individual PFCAs and PFSAs in the C4−C9 range[38−40] and nonlinear structures,[41−43] there has been little information available regarding the reactivity of many common PFASs such as fluorotelomers[29,30,34,37] and short-chain acids.[36,44] It is thus imperative to obtain a thorough understanding of the structure−reactivity relationship for (1) developing and assessing technologies to treat a broad spectrum of PFASs already released into the environment and (2) designing or modifying fluorochemical formulations to prevent future release of highly recalcitrant PFASs.

Hydrated electrons (e_{aq}^-) can be generated from H_2O or specific chemicals under UV irradiation.[45,46] Being highly reactive in reduction reactions, the e_{aq}^- has demonstrated excellent performance in cleaving C−F bonds. Since the pioneering work by Park et al.,[40] recent studies have investigated different e_{aq}^- source chemicals (e.g., iodide,[40] sulfite,[47] and indole[48]), e_{aq}^- generation strategies,[49] and UV irradiation[50,51] for the defluorination of PFOA and PFOS in aqueous solutions. At ambient temperature and in slightly basic solution (i.e., pH 9−10), a significant portion (50−90%) of C−F bonds can be cleaved from legacy PFOA[47] and PFOS[52] and the emerging GenX.[41] The dominant reactive species in the recently reported plasmatic defluorination is also e_{aq}^-.[26] Still, the feasibility of treating a wide spectrum of PFASs with e_{aq}^- and the underlying structure−reactivity relationship remain unknown. Herein, we report on a series of unexplored but critical trends in the structural dependence for PFAS defluorination. By examining a broad collection of 34 PFAS structures with various head groups and chain lengths, this study provides comprehensive mechanistic insights, and will significantly contribute to the advancement of technologies and strategies for PFASs remediation and management.

MATERIALS AND METHODS

Detailed information on chemicals and the preparation of PFAS stock solutions are described in the Supporting Information (SI). For the photochemical PFAS defluorination, a 600 mL solution containing 25 μM PFAS, 10 mM Na_2SO_3, and 5 mM $NaHCO_3$ (pH 9.5, adjusted by 1 M NaOH) was loaded in a closed-system photoreactor (cooled with 20 °C circulating water). The 18 W low-pressure mercury lamps (254 nm narrow band irradiation) were used for all reactions. Aliquots of solution were taken at time intervals for up to 48 h. Detailed reaction setup and rationales for the selected experimental conditions are described in the SI. The concentration of fluoride ion (F^-) released from PFASs was determined by an ion selective electrode (ISE). The accuracy of F^- measurement by the ISE in the solution matrix was validated by standard calibration and ion chromatography. The concentration of PFAS parent compounds was determined with liquid chromatography−triple quadrupole mass spectrometry (LC−MS/MS). Transformation product analyses were conducted by liquid chromatography−high resolution mass spectrometry (LC−HRMS). Full details of sample analysis are described in the SI. Theoretical calculations were performed according to the method used by Liu et al.[42] with details found in the SI.

RESULTS AND DISCUSSION

Decay and Defluorination of PFASs. *Perfluorocarboxylic Acids (PFCAs).* Figure 2a shows the decay of n = 1−10 PFCAs ($C_nF_{2n+1}COO^-$). Except for CF_3COO^-, the decay of PFCAs was complete within 8 to 12 h. Based on the concentration of F^- released from the PFAS molecules into the aqueous solution, the *overall* defluorination ratio (deF%) is defined in Equation 1):

$$\textit{overall}\ \text{deF\%} = \frac{C_{F^-}}{C_0 \times N_{C-F}} \times 100\% \quad (1)$$

where C_F^- is the molar concentration of F^- ion released in solution, C_0 is the initial molar concentration of the parent PFAS, and N_{C-F} is the number of C−F bonds in the parent PFAS molecule. The deF% for n = 2−10 PFCAs gradually leveled off to ~55% within 24 to 48 h (Figure 2b and Table 1). LC−MS/MS quantification of shorter-chain PFCAs and LC−HRMS analysis of partially defluorinated products did not fully close the mass balance with the identified charged intermediates and end products (see *PFAS Degradation Product*

DOI: 10.1021/acs.est.8b06648
Environ. Sci. Technol. 2019, 53, 3718−3728

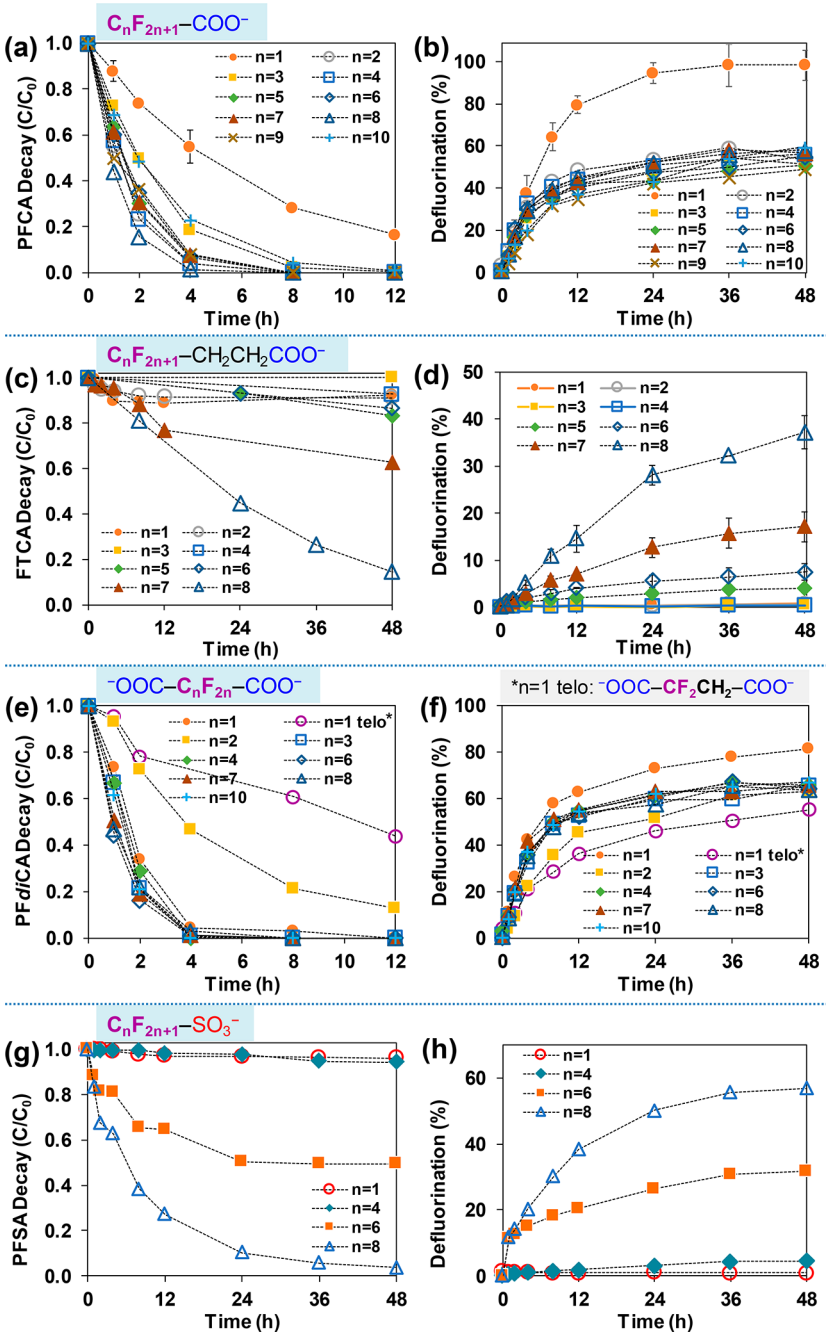

Figure 2. Time profiles for PFAS parent compound decay and defluorination. Reaction conditions: PFAS (0.025 mM), Na_2SO_3 (10 mM), carbonate buffer (5 mM), 254 nm irradiation (18 W low-pressure Hg lamp), pH 9.5 and 20 °C. Full degradation profile for TFA (n = 1 PFCA) is shown in Figure 6.

Analysis section). A surprising result is the 100% defluorination from trifluoroacetate (TFA, CF_3COO^-), while the rate of its degradation was slower than all $n \geq 2$ PFCAs. The contrasting results between n = 1 TFA and $n \geq 2$ PFCAs suggest new mechanistic insights (to be discussed in later sections). Transformation product analysis and discussion of degradation pathways for all PFAS categories examined in this study are presented in later sections.

Fluorotelomer Carboxylic Acids (FTCAs). We extended the investigation from PFCAs ($C_nF_{2n+1}COO^-$) to FTCAs (C_nF_{2n+1}–CH_2CH_2–COO^-) since a large variety of PFASs synthesized via telomerization contains one or more –CH_2– groups between the fluoroalkyl chain and the headgroup (Figure 1).[53] In comparison to PFCAs, the presence of –CH_2CH_2– in FTCAs resulted in significant persistence and dependence on C_nF_{2n+1} length for both parent compound decay (Figure 2c) and F^- release (Figure 2d and Table 1). Significant degradation was observed only for $n \geq 5$ FTCAs. After 48 h, the highest *overall* deF% was 37% for C_8F_{17}–CH_2CH_2–COO^-. This ratio was lower than those for the PFCAs either with the same length of fluorocarbon chain, $C_8F_{17}COO^-$ (58%) or with the same length of the whole molecule, C_8F_{17}–CF_2CF_2–COO^- (59%). Because a significant portion of the FTCA parent compounds still remained, the *molecular* deF% that considers the degraded portion (DG) of the parent compound is defined in Equation 2:

DOI: 10.1021/acs.est.8b06648
Environ. Sci. Technol. 2019, 53, 3718–3728

Table 1. Overall Defluorination Ratio of PFASs in Variable Fluoroalkyl Chain Lengths after 48 h of Reaction.[a]

chain length (n)	$F(CF_2)_n$–COOH	HOOC–$(CF_2)_n$–COOH	$F(CF_2)_n$–CH_2CH_2–COOH	$F(CF_2)_n$–SO_3H
1	98.2 ± 5.0	81.4 ± 4.2	0.73 ± 0.11	0.94 ± 0.18
2	53.3 ± 4.9	63.2 ± 4.3	0.94 ± 0.16	N/A[b]
3	51.1 ± 8.0	65.5 ± 4.4	1.1 ± 0.1	N/A[b]
4	56.1 ± 4.7	65.8 ± 2.1	0.71 ± 0.15	4.6 ± 0.8
5	51.0 ± 4.4	N/A[b]	4.1 ± 0.2	N/A[b]
6	55.1 ± 1.6	64.3 ± 2.2	7.4 ± 1.8	31.8 ± 0.8
7	56.5 ± 2.4	65.7 ± 3.9	17.1 ± 3.2	N/A[b]
8	58.2 ± 1.2	63.6 ± 2.7	33.4 ± 1.0	57.0 ± 1.2
9	49.1 ± 6.4	N/A[b]	N/A[b]	N/A[b]
10	59.5 ± 0.6	67.0 ± 0.5	N/A[b]	N/A[b]

[a]Reaction conditions: PFAS (0.025 mM), Na_2SO_3 (10 mM), carbonate buffer (5 mM), 254 nm irradiation (18 W low-pressure Hg lamp) at pH 9.5 and 20 °C. Errors indicate standard deviation of triplicate reactions. [b]Data not available because the chemical was commercially unavailable, too costly to afford, or not readily soluble in water (for long-chain structures).

$$\textit{molecular}\ \text{deF\%} = \frac{\textit{overall}\ \text{deF\%}}{\text{DG}} \quad (2)$$

For the three relatively long-chain FTCAs (n = 6, 7 and 8) that showed both significant parent compound decay (15%, 37%, and 85%, respectively) and *overall* deF% (7.4%, 17%, and 37%, respectively) after 48 h, their corresponding *molecular* deF% are similar (49%, 46%, and 44% respectively). The results suggest that while FTCA parent compounds are much more recalcitrant than PFCAs, (1) longer C_nF_{2n+1} in FTCAs provide higher reactivity, and (2) the reaction intermediates from the decayed portion of FTCAs provided ~50% defluorination in a relatively fast manner, regardless of the recalcitrance of the parent FTCAs.

Per- and Polyfluoro Dicarboxylic Acids (PFdiCAs). The comparison between PFCAs and FTCAs has clearly suggested that the direct linkage between $-COO^-$ and C_nF_{2n+1} promotes defluorination. We further examined such effects in PFdiCAs ($^-OOC-C_nF_{2n}-COO^-$), which have also been detected recently in water environments.[34] As shown in Figure 2e, the decay of parent PFdiCA compounds (n = 3–10) were complete within 4–8 h. The rates are faster than those for PFCAs (8–12 h, Figure 2a). The *overall* deF% at 48 h (identical to the *molecular* deF%, since the parent compound decay was complete for all PFCAs and PFdiCAs) were ~67% regardless of C_nF_{2n} length (Figure 2f and Table 1) and deeper than those for PFCAs (~55%). Similar to the case of CF_3COO^-, for $^-OOC-CF_2CF_2-COO^-$ (n = 2) where each CF_2 is directly linked to $-COO^-$, its decay and defluorination were significantly slower than long-chain PFdiCAs. Interestingly, the rate of decay for $^-OOC-CF_2-COO^-$ (n = 1) was similar to other long-chain PFdiCAs while the deF% was higher than all other PFdiCAs. However, the deF% was limited to 81% in comparison to the 100% for CF_3COO^-. In comparison to perfluorinated PFdiCA structures, retarded decay and defluorination of $^-OOC-CF_2-CH_2-COO^-$ was observed (the "n = 1 telo*" in Figure 2e and f).

Perfluoroalkanesulfonic Acids (PFSAs). With the different effects of $-COO^-$ versus $-CH_2CH_2-COO^-$ on defluorination observed, it is intriguing to also probe the effect of $-SO_3^-$ on the treatment of $C_nF_{2n+1}SO_3^-$. Like the FTCAs, the decay (Figure 2g) and defluorination (Figure 2h and Table 1) of n = 4, 6, and 8 PFSAs showed significant dependence on chain length. This trend agrees with the study by Park et al.,[40] where iodide was used as the source of e_{aq}^-. In contrast to the almost complete defluorination of CF_3COO^-, the n = 1 $CF_3SO_3^-$ showed negligible decay and defluorination. Thus, the effect of $-SO_3^-$ on e_{aq}^- mediated defluorination is vastly different from that of $-COO^-$. Similar with the FTCAs, n = 6 and n = 8 PFSAs that showed significant parent compound decay (50% and 96%, respectively) and *overall* deF% (32% and 57%, respectively) exhibited similar *molecular* deF% (64% and 59%, respectively) after 48 h. Similar results on PFOS degradation were found in a study by Sun et al.,[49] where ~50% *molecular average* deF% was observed for reactions in various experimental settings. Thus, like FTCAs, although PFSAs with different chain lengths showed varying rates of parent compound decay, the defluorination from the decayed portion was relatively fast toward a similar extent.

Structural Effects and Mechanistic insights on PFAS Degradation. The experimental results have clearly shown that the rate of PFAS decay and defluorination highly depend on both the headgroup and the fluoroalkyl chain length. The direct linkage between the fluoroalkyl chain and $-COO^-$ seems critical for a fast defluorination reaction. As shown in Figure 2, the decay of all $n \geq 2$ $C_nF_{2n+1}COO^-$ proceeded at a faster pace than F^- release, indicating that the degradation of reaction intermediates was slower than the transformation of parent structures. In contrast, the decay of FTCA and PFSA parent structures (e.g., n = 6/7/8 $C_nF_{2n+1}-CH_2CH_2-COO^-$ and n = 6/8 $C_nF_{2n+1}SO_3^-$) limits the processes of F^- release, suggesting that the degradation of reaction intermediates was faster than the decay of parent structures. Results from a series of theoretical calculations and product analyses suggest deeper insights into the mechanisms and pathways for the reductive defluorination mediated by e_{aq}^-.

Theoretical Calculations of C–F Bond Dissociation Energies (BDEs). The C–F BDEs in all PFAS structures were calculated with density functional theory (DFT) in conjunction with an SDM polarizable continuum model (see the SI for computational details). The full collection of BDE data is summarized in SI Tables S1–S5, and representative results are shown in Figure 3. As expected, BDEs of all primary C–F bonds (i.e., bonds on the terminal $-CF_3$; 117.8–123.4 kcal mol^{-1}) are higher than all secondary C–F bonds (i.e., bonds on $-CF_2-$; 106.4–113.6 kcal mol^{-1}).[42] In general, lower BDEs for both primary and secondary C–F bonds are observed in PFASs with longer fluoroalkyl chains (Figure 3a–c and h, i). This trend may explain why the rate of parent compound degradation was faster for longer chain FTCAs and PFSAs, where more $-CF_2-$ functional groups in the middle of the fluoroalkyl chains have low BDEs (typically ≤107.5 kcal mol^{-1}). We note that the "decay" of a parent compound only needs one bond to be cleaved. Considering our calculation results and a previous theoretical study[54] where the central $-CF_2-$ in a fluoroalkyl chain was found to have the highest affinity to the "extra" electron (i.e., e_{aq}^- in this study), we propose that the first defluorination occurs at a middle $-CF_2-$ group in long-chain (typically $n \geq 5$) FTCA and PFSA structures.

As for PFCAs and PFdiCAs, the C–F BDEs for the α-position $-CF_2-$ (i.e., adjacent to $-COO^-$; 106.5–107.3 kcal mol^{-1}, Figure 3e and g) are all lower than those of α-position C–F bonds in FTCAs and PFSAs (109.2–113.6 kcal mol^{-1}).

DOI: 10.1021/acs.est.8b06648
Environ. Sci. Technol. 2019, 53, 3718–3728

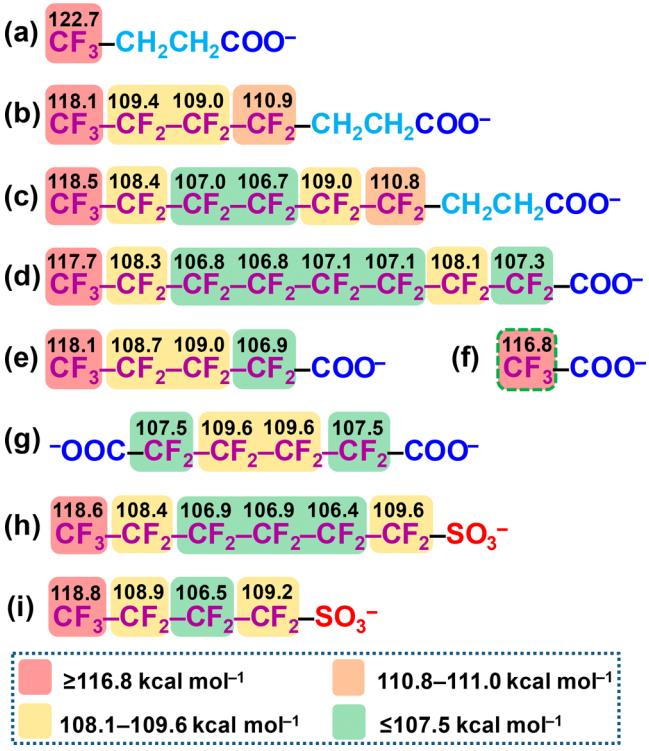

Figure 3. Calculated C–F BDEs (kcal mol^{-1}) of selected PFASs at the B3LYP-D3(BJ)/6-311+G(2d,2p) level of theory. Calculation results for all structures are tabulated in SI Tables S1–S5.

From the experimental results, it appears that the α-position C–F bonds may contribute to the high reactivity of PFCAs. This is also supported by the faster decay and higher defluorination ratio from PFdiCAs rather than from PFCAs by having two $-COO^-$ head groups (Figure 3g vs e) and lacking primary C–F bonds. However, the similarly low BDEs for β-position C–F bonds in PFSAs (Figure 3i vs e) did not promote the reaction of short-chain $C_4F_9-SO_3^-$ structure (Figure 2g), indicating that the BDE of individual bonds may not be the only factor determining the rate of reaction.

Spontaneous Bond Cleavage in Electron-Added PFAS Radical Anion Structures. Since the defluorination of PFASs occurred upon the reaction with e_{aq}^-, we further conducted DFT calculations of C–F BDEs of the radical anion after the original PFAS anion received an "extra" electron:

$$C_nF_{2n+1}-COO^- + e_{aq}^- \rightarrow C_nF_{2n+1}-COO\bullet^{2-} \quad (3)$$

To our surprise, when a geometry optimization was applied to the radical anions of PFCAs, FTCAs, and PFSAs, a spontaneous bond stretching was observed (Figure 4). One α-position C–F bond in $C_6F_{13}-COO^{\bullet 2-}$ was stretched to 4.5 Å, which indicates bond cleavage. The $C_4F_9-COO^{\bullet 2-}$ and $C_8F_{17}-COO^{\bullet 2-}$ analogs showed similar bond cleavage of α-position C–F bonds (SI Figure S1). Hence, while the spontaneous bond cleavage makes it difficult to calculate BDEs in the unstable PFAS$^{\bullet 2-}$, the calculation results for the original PFCA anions are informative for mechanistic interpretation or prediction of the reactions with e_{aq}^-. As for FTCA radical anions, C–F bond stretching was observed in the middle of the fluorocarbon chain in $C_6F_{13}-CH_2CH_2-COO^{\bullet 2-}$ (Figure 4). Although n = 4 and n = 8 FTCA radical anions did not show similar C–F bond stretching, the result from the n = 6 structure has already suggested the possibility of

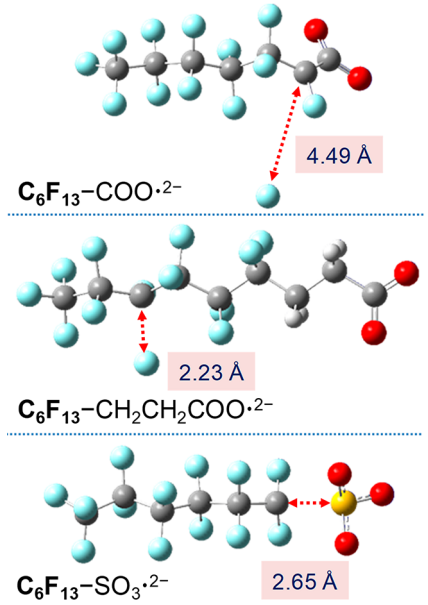

Figure 4. Geometry-optimized structure of the adducts of the three n = 6 PFAS anions with an e_{aq}^- (PFAS$^{\bullet 2-}$) at the B3LYP-D3(BJ)/6-311+G(2d,2p) level of theory.

middle-chain C–F bond cleavage upon the reaction between FTCA anions and e_{aq}^- (SI Figure S3). The C–S bond stretching was observed for n = 4, 6, and 8 $C_nF_{2n+1}-SO_3^{\bullet 2-}$, indicating the dissociation of the sulfonate group upon the reaction between PFSA anions and e_{aq}^- (SI Figure S2). This result agrees with the previous mechanistic interpretation on PFOS degradation, where the C–S bond cleavage led to the formation of PFOA.[50] However, we highlight that calculations of C–F and C–S bond cleavage are not the sole degradation pathways for each category of PFASs (see below).

PFAS Degradation Product Analysis. In previous studies on PFOA/PFOS defluorination with e_{aq}^-, the total concentration of all shorter-chain PFCA products contributed to <3% of the initial PFOA/PFOS concentration.[47,50] Here we used suspect screening of LC–HRMS data to identify other plausible products beyond the shorter-chain PFCAs (all results collected in SI Tables S6–S18). As shown in Figure 5a and SI Table S8, the degradation of $C_7F_{15}-COO^-$ (PFOA, initial concentration 25 μM) produced at least two partially defluorinated products, $C_7F_{14}H-COO^-$ and $C_7F_{13}H_2-COO^-$, with the highest peak area of 2.42 × 10^8 at 4 h and 3.63 × 10^7 at 48 h, respectively. As analytical standards are not available for accurate quantification of those two products, the peak area is used to roughly estimate the relative abundance in comparison to the parent compound (assuming the ionization efficiencies vary within 1 order of magnitude). From the data, the max. peak intensities for $C_7F_{14}H-COO^-$ (upon one H/F exchange) and $C_7F_{13}H_2-COO^-$ (upon two H/F exchanges) were 1 and 2 orders of magnitude lower than the parent $C_7F_{15}-COO^-$, respectively. We point out that as reaction intermediates are subject to further degradation, the accumulative generation of these species could be much higher than the maximum concentration observed at a single time point. The shorter-chain PFHpA anion $C_6F_{13}-COO^-$ was also observed with the max. concentration of 265 nM at 1 h, corresponding to 1.1% of the initial PFOA. Low-intensity peaks (<5 × 10^6 but higher than the arbitrary 10^5 threshold used for product identification) for other anions were also

DOI: 10.1021/acs.est.8b06648
Environ. Sci. Technol. 2019, 53, 3718–3728

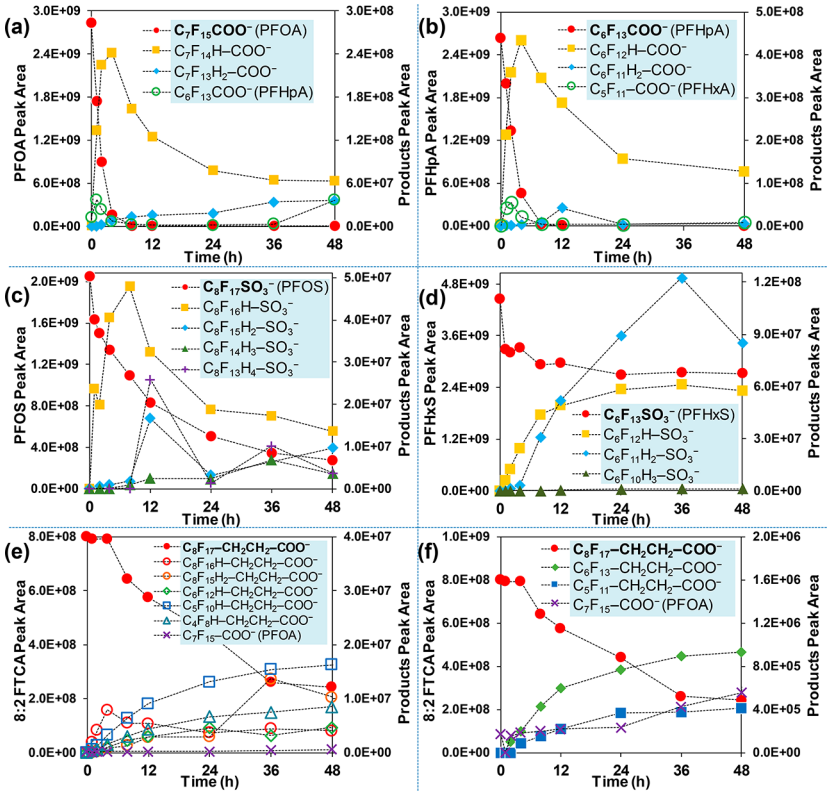

Figure 5. Representative degradation products from (a) PFOA, (b) PFHpA, (c) PFOS, (d) PFHxS, and (e+f) n = 8 FTCA. All detected species including those in low intensities are summarized in SI Tables S6–S18.

observed (summarized in SI Table S8), such as $C_7F_{12}H_3-COO^-$, $C_7F_{11}H_4-COO^-$, and $C_7F_9H_6-COO^-$ (i.e., three, four, and six H/F exchanges from PFOA), as well as $C_6F_{12}H-COO^-$ and $C_6F_9H_4-COO^-$ (i.e., one and four H/F exchanges from the product PFHpA), and even shorter-chain $C_5F_{10}H-COO^-$ (i.e., one H/F exchange from the product PFHxA). The detection of products with more than two H/F exchanges from PFOA and PFHpA suggests that, the weak C–F bonds in the middle of the long fluoroalkyl chain in PFCAs are also susceptible to cleavage.

To further understand the fate of the chain-shortened PFHpA generated from PFOA degradation, we also characterized the products from the degradation of pure PFHpA (Figure 5b). Very similar to the degradation of PFOA, three major products from PFHpA are single-H/F-exchange product $C_6F_{12}H-COO^-$ (peaked at 4 h), double-H/F-exchange product $C_6F_{11}H_2-COO^-$ (peaked at 12 h), and the shorter-chain PFHxA (peaked at 2 h, 1.3% of the added PFHpA). Further investigations of longer (e.g., PFDA and PFNA) and shorter PFCAs (e.g., PFHxA) also revealed very similar trends (SI Figure S4 and Tables S6–S10). From the formation curves of the three major products, the maximum intensity of shorter-chain PFCAs appeared earlier than those of the two H/F exchange products. Therefore, the degradation of PFCAs have at least two independent pathways, (i) H/F exchange without chain-shortening and (ii) formation of shorter-chain PFCAs.

Specifically, the $C_nF_{2n-1}H_2-COO^-$ built up in the reactions of all PFCAs (Figure S4). We propose that the most probable structure for this product is $C_{n-1}F_{2n-1}-CH_2-COO^-$ (i.e., double H/F exchanges on the α–position carbon) for the following reasons. First, according to the calculated C–F BDEs in the $C_nF_{2n+1}-COO^-$ and the spontaneous C–F cleavage from the e_{aq}^- added $C_nF_{2n+1}-COO^{\bullet 2-}$, the first H/F exchange is highly likely to occur at the α-position. Second, if the first C–F bond is replaced by a C–H bond, the remaining C–F bond on the same carbon is significantly weakened (SI Text S1) to become even more susceptible for the following H/F exchange. Third, as suggested by the recalcitrant decay of FTCAs, the separation of the fluoroalkyl chain and the $-COO^-$ with one $-CH_2-$ linker is the most probable structure showing recalcitrance. To further test the hypothesis regarding the slow reaction of $C_nF_{2n+1}-CH_2-COO^-$ with only one $-CH_2-$ linker, we investigated a commercially available structure, $CF_3-CH_2-COO^-$ (structural analogues with longer fluorocarbon chains were not available to test). Compared to the perfluorinated $CF_3-CF_2-COO^-$ (53% defluorination) and CF_3-COO^- (100% defluorination), the structure with a single $-CH_2-$ linker indeed showed very sluggish reactivity with only 2.2% defluorination measured after 48 h.

As for PFSAs, we analyzed the products from the reactions of PFOS and PFHxS that exhibited significant decay and defluorination. Results suggest that the calculated spontaneous C–S cleavage is one of the two reaction pathways, the other being the H/F exchange without chain shortening. For PFOS degradation, products with one ($C_8F_{16}H-SO_3^-$), two ($C_8F_{15}H_2-SO_3^-$), three ($C_8F_{14}H_3-SO_3^-$), and four H/F exchanges ($C_8F_{13}H_4-SO_3^-$) on the eight-carbon PFOS backbone were observed in significant abundance (Figure 5c and SI Table S11). The intensity of those four peaks were 2 orders of magnitude lower than the parent PFOS. Meanwhile, a series of PFCAs (from PFOA to PFBA) were also observed with low intensities (SI Table S13). However, these PFCAs showed a similar abundance in the product mixture from PFOS degradation. For comparison, in the experiments

DOI: 10.1021/acs.est.8b06648
Environ. Sci. Technol. 2019, 53, 3718–3728

Scheme 1. Proposed Overall Reaction Mechanisms for PFAS Degradation and Defluorination

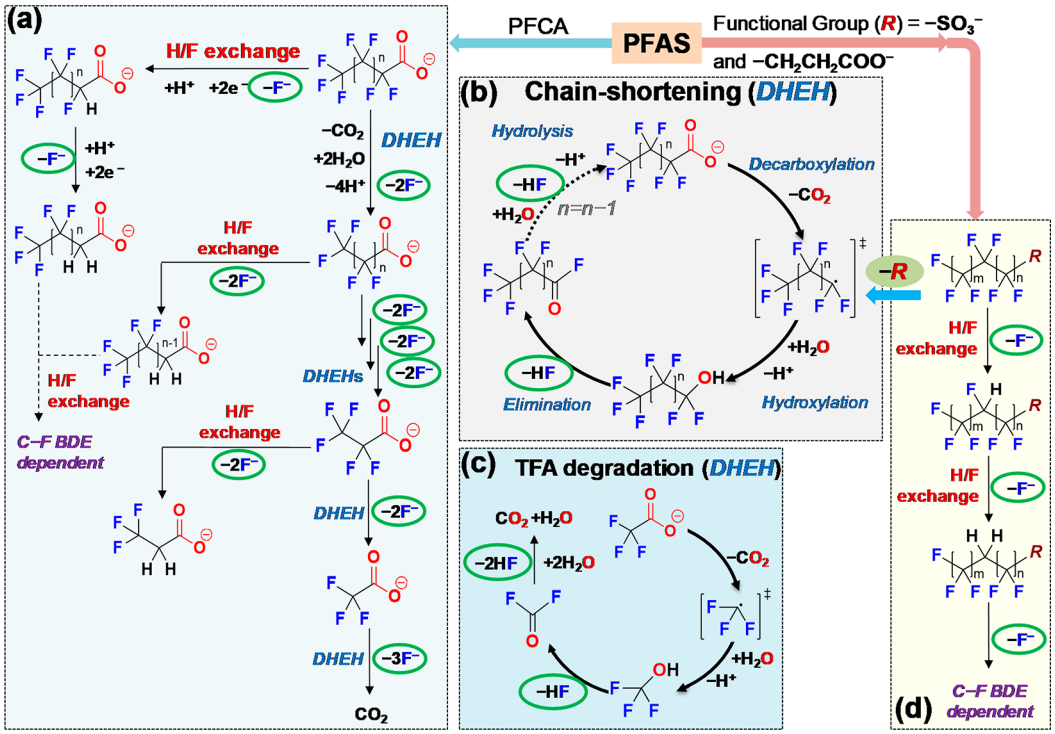

starting from individual PFCAs, the chain-shortened daughter PFCA was in much lower abundance than the parent PFCA (Figure 5a and b). Thus, the shorter-chain PFCAs observed in PFOS degradation were not generated from the sequential chain-shortening from PFOA. We found that the commercial PFOS reagent actually contained a small portion of shorter-chain PFSAs such as PFHpS, PFHxS, and PFBS, and their corresponding H/F exchange products were also detected (SI Table S12). Thus, the formation of PFCAs in relatively high abundance for all chain lengths might be attributed to the C−S cleavage of the corresponding PFSAs. Similar product profiles were observed for PFHxS degradation (Figure 5d and SI Tables S14−16).

The product analysis on the degradation of the telomeric $C_8F_{17}-CH_2CH_2-COO^-$ (Figure 5e and f; SI Tables S17 and S18) also suggested two reaction pathways. First, H/F exchange products were observed, for example, $C_8F_{16}H-CH_2CH_2-COO^-$ (peaked at 4 h) and $C_8F_{15}H_2-CH_2CH_2-COO^-$ (peaked at 36 h). Based on our calculation results (Figure 3 and SI Table S3), the most probable H/F exchange should occur in the middle of the long fluoroalkyl chain. Recall that the decay of shorter-chain FTCAs was very sluggish, most probably due to the lack of low BDE C−F bonds. However, the formation of $C_9F_{12}H_5O_2^-$, $C_8F_{10}H_5O_2^-$, and $C_7F_8H_5O_2^-$ (most probably with the structure $C_nF_{2n}H-CH_2CH_2-COO^-$) cannot be explained at this moment. Unlike PFSA reagents that contain multiple shorter-chain impurities, the shorter-chain FTCAs were not detected in t = 0 samples (SI Table S17), indicating that they were indeed generated from the chain-shortening of the n = 8 FTCA. It is not yet clear how the fluorocarbon chain was shortened without losing the $-CH_2CH_2-COO^-$ headgroup. Still, low intensities of PFCAs were observed (e.g., PFBA shown in SI Table S18), indicating the dissociation of $-CH_2CH_2-COO^-$ as the second mechanism for FTCA degradation.

Overall Reaction Mechanisms. Based on the experimentally observed PFAS decay and defluorination, DFT calculations, and degradation product analyses, the reaction mechanisms are summarized in Scheme 1. PFCAs ($C_nF_{2n+1}-COO^-$) undergo two pathways upon reaction with e_{aq}^- (Scheme 1a). First, two H/F exchanges occur sequentially on the α-position and yield $C_{n-1}F_{2n-1}-CH_2-COO^-$, which has high recalcitrance. If the fluorocarbon chain is long, it is also possible to have additional C−F bond cleavage from middle $-CF_2-$ groups. Second, shorter-chain PFCAs are generated most probably from a decarboxylation mechanism (Scheme 1b), yielding an unstable perfluorinated alcohol ($C_nF_{2n+1}-OH$) that is subject to HF elimination.[55] The resulted acyl fluoride is hydrolyzed to release the second fluoride ion, and the shorter-chain PFCA ($C_{n-1}F_{2n-1}-COO^-$) thus forms and enters the next reaction cycle.[56] This decarboxylation−hydroxylation−elimination−hydrolysis (DHEH) pathway has been mainly inferred from prior literature[47,50,55,56] and few recent studies have provided further insights on the stability of perfluorinated alcohol. However, there is some indirect evidence to support the DHEH mechanism. First, perfluorinated $C_nF_{2n+1}-OH$ has been rarely reported as a bulk chemical. Instead, the widely used fluorinated alcohols are telomeric $C_nF_{2n+1}-CH_2-OH$.[57,58] This fact may reflect the instability of $C_nF_{2n+1}-OH$. Second, an analogous structure, FCH_2-OH, has only been observed spectroscopically under low temperatures in a mixture of HCOH and HF (i.e., $FCH_2-OH \leftrightarrow HCOH + HF$).[59] This equilibrium supports the mechanism of HF elimination from structures with one −F and one −OH on the same carbon.

We also found that the 100% defluorination of TFA (CF_3-COO^-) strongly supports this DHEH mechanism (Scheme 1c). First, TFA only has three high-BDE primary C−F bonds (Figure 3f) so that a direct C−F bond cleavage seems less likely. Second, our experimental results for DFA (CF_2H-

DOI: 10.1021/acs.est.8b06648
Environ. Sci. Technol. 2019, 53, 3718−3728

COO^-) and MFA (CFH_2-COO^-) defluorination indicate that the previously proposed stepwise defluorination mechanism for TFA is less likely.[60] As shown in Figure 6, although

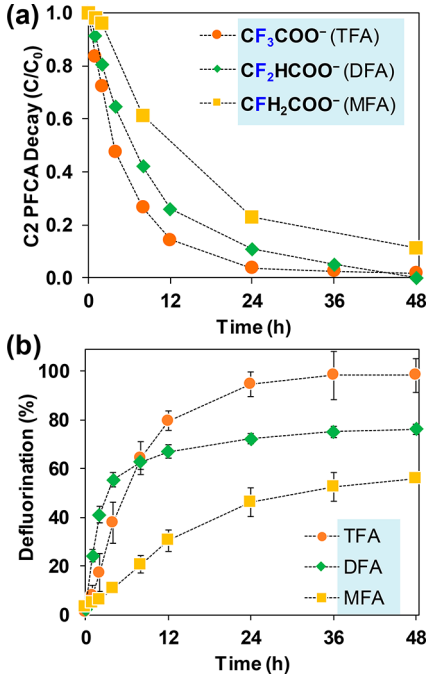

Figure 6. Time profiles for the (a) decay and (b) defluorination of the three fluorinated acetic acid derivatives. Reaction conditions are the same as indicated in Figure 2.

complete decay of fluorinated acetates was observed, the maximum defluorination from DFA and MFA was 78% and 57%, respectively. Hence, the stepwise reaction of TFA → DFA → MFA would not lead to a 100% defluorination as observed from TFA. The incomplete defluorination from MFA and DFA might be attributed to the rapid volatilization of FCH_2-OH[59] and F_2CH-OH prior to HF elimination. Third, the closely synchronized profiles of decay and defluorination of TFA suggest that the change of TFA parent structure triggered rapid liberation of all three F^- ions. While other reaction mechanisms have not been identified, the DHEH pathway is the most probable mechanism for PFCA chain-shortening and the accompanying F^- release.

If the PFCA degradation followed the single pathway of chain-shortening through the DHEH pathway, a complete defluorination would have been observed. Thus, the ~55% max. defluorination from all $n \geq 2$ $C_nF_{2n+1}-COO^-$ is attributed to other reaction pathways via H/F exchange. Assuming that only these two mechanisms apply to the simple $CF_3CF_2COO^-$ structure, a DHEH as the first step will generate two F^- and CF_3COO^-, which can be fully defluorinated in the second DHEH (deF% = 100%). Meanwhile, the H/F exchange as the first step will accumulate $CF_3CH_2COO^-$ with high recalcitrance (deF% = 40%). Thus, the overall ~55% defluorination from $CF_3CF_2COO^-$ indicates a 75% probability for H/F exchange and 25% probability for DHEH as the first step. We also note that each shorter-chain PFCA product will also undergo the two competing pathways, leading to the accumulation of H-containing structures with high recalcitrance. For long-chain PFCAs and intermediates, H/F exchange in the middle of fluoroalkyl chain is also possible (SI Table S8).

The presence of one more $-COO^-$ terminal group in PFdiCAs (~67% max. defluorination) enables degradation from the other side of molecule. Either α-position H/F exchange or DHEH pathways from the second $-COO^-$ would lead to higher deF% than PFCAs, which have the most recalcitrant $-CF_3$ on the other end. In addition, our results do not support the previously proposed PFOA degradation mechanism, where $C_nF_{2n+1}-CH_2-COO^-$ (generated from $C_nF_{2n+1}-CF_2-COO^-$) decomposes to three pieces, $\bullet C_nF_{2n+1}$, $:CH_2$, and $\bullet COO^-$, and then the $\bullet C_nF_{2n+1}$ and $\bullet COO^-$ recombines into the shortened $C_nF_{2n+1}-COO^-$.[60] If this mechanism was dominant, the degradation of $CF_3-CH_2-COO^-$ would be fast, and the degradation of all $n \geq 2$ PFCAs would be shortened stepwise to TFA and yield 100% defluorination. We also note that even if the three-piece decomposition could occur, the chance of recombination of the two radicals in very low concentration (e.g., sub-μM level) in water would be trivial.

As for PFSAs and FTCAs, the first reaction pathway is H/F exchange on relatively weak C−F bonds, which mainly occur in the middle of the long-chain structures (Scheme 1d). We add that if the middle-chain $-CF_2-$ is reduced to $-CH_2-$, the long fluorocarbon chain is thus divided into two short fluorocarbon chains, where most C−F bonds will have high BDEs (Figure 3b vs c). The other pathway is the cleavage of the head groups and the formation of PFCAs following either the H/F exchange or the DHEH mechanism. The similar *molecular* deF% values from the decayed portion of PFSAs (59−64%) and FTCAs (44−49%) in variable lengths support this speculation, which warrants further investigation.

According to the MS peak areas of the parent compound and the identified degradation products (assuming they have similar ionization efficiency), the F mass balance seems not yet closed. This is probably because (1) the ionization efficiency may vary significantly for different products, leading to inaccurate estimation of product abundances, (2) a portion of degradation products might have lost the charged headgroup and thus escaped from MS detection,[42,43] and/or (3) novel products generated from other reaction pathways were not identified by the screening of suspect products from chain shortening and H/F exchange. The mechanisms for some reactions still remain elusive. For example, FTCA chain shortening occurred with the $-CH_2CH_2-COO^-$ headgroup remaining. In the degradation of PFOS and PFHxS, high intensities of H/F exchange structures ($C_4F_8H-SO_3^-$ and $C_3F_6H-SO_3^-$) were observed (SI Tables S12 and S15) despite that PFBS and PFPrS are highly recalcitrant. These results suggest that there are still unknown degradation mechanisms involved in PFAS degradation with e_{aq}^-. However, since this treatment strategy is not very effective to short fluorocarbon chains that are not directly linked to $-COO^-$, mechanistic investigation on the unfavorable pathways goes beyond the focus of this study. Instead, priority of research should be given to further improving the rate and extent of the degradation of recalcitrant PFAS structures.

Critical Implications to PFASs Remediation and Management. A series of critical environmental implications can be explicitly made from the findings of this study. First, the direct linkage between fluoroalkyl chain and $-COO^-$ is highly beneficial for reductive defluorination with e_{aq}^-. From the remediation perspective, chemical[61] and biological[62] trans-

DOI: 10.1021/acs.est.8b06648
Environ. Sci. Technol. 2019, 53, 3718−3728

formation of telomeric structures are expected to produce PFCAs for significantly enhanced defluorination efficiency of the following treatment step with e_{aq}^-. From the management perspective, perfluorinated sulfonates with short fluoroalkyl chains[36] should be applied with caution due to their sluggish reactivity with e_{aq}^- and their recalcitrance to oxidation. We accentuate that the future design of mixed AFFF formulation should seriously consider the treatability of specific PFAS structures to avoid the recalcitrance against remediation efforts. Second, further elevated defluorination can be expected from the optimization of reaction conditions (e.g., selection of chemicals for e_{aq}^- generation,[49,63] UV energy and intensity,[50,51] and the use of heterogeneous materials[48]) and the development of technologies with novel working principles.[24,25] Lastly, since other emerging technologies such as electrochemical and plasmatic treatment have also observed slower degradation of C6 PFHxS than C8 PFOS,[15,26] we emphasize the necessity of examining a variety of representative structures as the PFAS contamination in the real world are usually present as a mixture of diverse structures.

■ ASSOCIATED CONTENT

Supporting Information

The Supporting Information is available free of charge on the ACS Publications website at DOI: 10.1021/acs.est.8b06648.

Additional tables, figures, discussions, and detailed experimental procedures (PDF)

■ AUTHOR INFORMATION

Corresponding Author

*E-mail: jyliu@engr.ucr.edu; jinyong.liu101@gmail.com.

ORCID

Yaochun Yu: 0000-0001-9231-6026

Bryan M. Wong: 0000-0002-3477-8043

Yujie Men: 0000-0001-9811-3828

Jinyong Liu: 0000-0003-1473-5377

Notes

The authors declare no competing financial interest.

■ ACKNOWLEDGMENTS

Financial support was provided by the UCR Initial Complement for J.L., UCR Collaborative Seed Grant for J.L., B.M.W., and L.X; the National Science Foundation (CHE-1709719 for J.L. and CHE-1709286 for Y.M. and Y.Y.), and the Strategic Environmental Research and Development Program (ER-1289 for J.L. and B.M.W, and ER-1497 for J.L.). M.J.B. received a scholarship from the UCR Water SENSE Integrative Graduate Education and Research Traineeship (IGERT) supported by NSF. UCR undergraduate researchers, Taylor Brantner, Robert Chavarria-Vivar, Vanessa Coria, Duy Dao, Maggy Harake, and Vivian Ngo provided technical assistance on photochemical reactions.

■ REFERENCES

(1) Xiao, F. Emerging poly-and perfluoroalkyl substances in the aquatic environment: A review of current literature. *Water Res.* **2017**, *124*, 482−495.

(2) Houde, M.; De Silva, A. O.; Muir, D. C.; Letcher, R. J. Monitoring of perfluorinated compounds in aquatic biota: An updated review: PFCs in aquatic biota. *Environ. Sci. Technol.* **2011**, *45* (19), 7962−7973.

(3) Environmental, U. S. Protection Agency. Revisions to the unregulated contaminant monitoring regulation (UCMR 3) for public water systems. *Fed. Reg.* **2012**, *77* (85), 26071−26101.

(4) Environmental, U. S. Protection Agency. Lifetime health advisories and health effects support documents for perfluorooctanoic acid and perfluorooctane sulfonate. *Fed. Reg.* **2016**, *81* (101), 33250−33251.

(5) Vermont Department of Health. Health Department Updates Health Advisory for PFAS. http://www.healthvermont.gov/media/newsroom/updated-pfas-health-advisory-july-10-2018.

(6) Massachusetts Department of Environmental Protection. MassDEP ORS Guideline for PFAS. https://www.mass.gov/files/documents/2018/06/11/orsg-pfas-20180608.pdf.

(7) New Jersey Drinking Water Quality Institute. Maximum Contaminant Level Recommendations for Perfluorononanoic Acid in Drinking Water: Basis and Background. https://www.nj.gov/dep/watersupply/pdf/pfna-recommend-final.pdf.

(8) North Carolina Department of Environmental Quality and North Carolina Department of Health and Human Services. Secretaries' Science Advisory Board Review of the North Carolina Drinking Water Provisional Health Goal for GenX. https://files.nc.gov/ncdeq/GenX/SAB/SAB-GenX-Report-draft-08-29-2018.pdf.

(9) Trojanowicz, M.; Bojanowska-Czajka, A.; Bartosiewicz, I.; Kulisa, K. Advanced Oxidation/Reduction Processes treatment for aqueous perfluorooctanoate (PFOA) and perfluorooctanesulfonate (PFOS)−A review of recent advances. *Chem. Eng. J.* **2018**, *336*, 170−199.

(10) Merino, N.; Qu, Y.; Deeb, R. A.; Hawley, E. L.; Hoffmann, M. R.; Mahendra, S. Degradation and removal methods for perfluoroalkyl and polyfluoroalkyl substances in water. *Environ. Eng. Sci.* **2016**, *33* (9), 615−649.

(11) Rahman, M. F.; Peldszus, S.; Anderson, W. B. Behaviour and fate of perfluoroalkyl and polyfluoroalkyl substances (PFASs) in drinking water treatment: A review. *Water Res.* **2014**, *50*, 318−340.

(12) Xiao, X.; Ulrich, B. A.; Chen, B.; Higgins, C. P. Sorption of poly- and perfluoroalkyl substances (PFASs) relevant to aqueous film-forming Foam (AFFF)-impacted groundwater by biochars and activated carbon. *Environ. Sci. Technol.* **2017**, *51* (11), 6342−6351.

(13) Boo, C.; Wang, Y.; Zucker, I.; Choo, Y.; Osuji, C. O.; Elimelech, M. High performance nanofiltration membrane for effective removal of perfluoroalkyl substances at high water recovery. *Environ. Sci. Technol.* **2018**, *52* (13), 7279−7288.

(14) Zhuo, Q.; Deng, S.; Yang, B.; Huang, J.; Yu, G. Efficient electrochemical oxidation of perfluorooctanoate using a Ti/SnO_2-Sb-Bi anode. *Environ. Sci. Technol.* **2011**, *45* (7), 2973−2979.

(15) Schaefer, C. E.; Andaya, C.; Burant, A.; Condee, C. W.; Urtiaga, A.; Strathmann, T. J.; Higgins, C. P. Electrochemical treatment of perfluorooctanoic acid and perfluorooctane sulfonate: Insights into mechanisms and application to groundwater treatment. *Chem. Eng. J.* **2017**, *317*, 424−432.

(16) Schaefer, C. E.; Choyke, S.; Ferguson, P. L.; Andaya, C.; Burant, A.; Maizel, A.; Strathmann, T. J.; Higgins, C. P. Electrochemical transformations of perfluoroalkyl acid (PFAA) precursors and PFAAs in groundwater impacted with aqueous film forming foams. *Environ. Sci. Technol.* **2018**, *52* (18), 10689−10697.

(17) Lin, H.; Niu, J.; Xu, J.; Huang, H.; Li, D.; Yue, Z.; Feng, C. Highly efficient and mild electrochemical mineralization of long-chain perfluorocarboxylic acids (C9−C10) by Ti/SnO_2−Sb−Ce, Ti/SnO_2−Sb/Ce−PbO_2 and Ti/BDD electrodes. *Environ. Sci. Technol.* **2013**, *47* (22), 13039−13046.

(18) Moriwaki, H.; Takagi, Y.; Tanaka, M.; Tsuruho, K.; Okitsu, K.; Maeda, Y. Sonochemical decomposition of perfluorooctane sulfonate and perfluorooctanoic acid. *Environ. Sci. Technol.* **2005**, *39* (9), 3388−3392.

(19) Vecitis, C. D.; Wang, Y.; Cheng, J.; Park, H.; Mader, B. T.; Hoffmann, M. R. Sonochemical degradation of perfluorooctanesulfonate in aqueous film-forming foams. *Environ. Sci. Technol.* **2010**, *44* (1), 432−438.

(20) Gole, V. L.; Fishgold, A.; Sierra-Alvarez, R.; Deymier, P.; Keswani, M. Treatment of perfluorooctane sulfonic acid (PFOS)

using a large-scale sonochemical reactor. *Sep. Purif. Technol.* **2018**, *194*, 104−110.
(21) Sahu, S. P.; Qanbarzadeh, M.; Ateia, M.; Torkzadeh, H.; Maroli, A. S.; Cates, E. L. Rapid degradation and mineralization of perfluorooctanoic acid by a new petitjeanite $Bi_3O(OH)(PO_4)_2$ microparticle ultraviolet photocatalyst. *Environ. Sci. Technol. Lett.* **2018**, *5* (8), 533−538.
(22) Li, X.; Zhang, P.; Jin, L.; Shao, T.; Li, Z.; Cao, J. Efficient photocatalytic decomposition of perfluorooctanoic acid by indium oxide and its mechanism. *Environ. Sci. Technol.* **2012**, *46* (10), 5528−5534.
(23) Ochiai, T.; Iizuka, Y.; Nakata, K.; Murakami, T.; Tryk, D. A.; Koide, Y.; Morito, Y.; Fujishima, A. Efficient decomposition of perfluorocarboxylic acids in aqueous suspensions of a TiO_2 photocatalyst with medium-pressure ultraviolet lamp irradiation under atmospheric pressure. *Ind. Eng. Chem. Res.* **2011**, *50* (19), 10943−10947.
(24) Zhang, K.; Huang, J.; Yu, G.; Zhang, Q.; Deng, S.; Wang, B. Destruction of perfluorooctane sulfonate (PFOS) and perfluorooctanoic acid (PFOA) by ball milling. *Environ. Sci. Technol.* **2013**, *47* (12), 6471−6477.
(25) Lu, M.; Cagnetta, G.; Zhang, K.; Huang, J.; Yu, G. Mechanochemical mineralization of "very persistent" fluorocarbon surfactants−6:2 fluorotelomer sulfonate (6:2 FTS) as an example. *Sci. Rep.* **2017**, *7*, 17180.
(26) Stratton, G. R.; Dai, F.; Bellona, C. L.; Holsen, T. M.; Dickenson, E. R.; Mededovic Thagard, S. Plasma-based water treatment: efficient transformation of perfluoroalkyl substances in prepared solutions and contaminated groundwater. *Environ. Sci. Technol.* **2017**, *51* (3), 1643−1648.
(27) Zhang, Z.; Chen, J. J.; Lyu, X. J.; Yin, H.; Sheng, G. P. Complete mineralization of perfluorooctanoic acid (PFOA) by γ-irradiation in aqueous solution. *Sci. Rep.* **2015**, *4*, 7418.
(28) Dombrowski, P. M.; Kakarla, P.; Caldicott, W.; Chin, Y.; Sadeghi, V.; Bogdan, D.; Barajas Rodriguez, F.; Chiang, S. Y. Technology review and evaluation of different chemical oxidation conditions on treatability of PFAS. *Remed. J.* **2018**, *28* (2), 135−150.
(29) Barzen-Hanson, K. A.; Roberts, S. C.; Choyke, S.; Oetjen, K.; McAlees, A.; Riddell, N.; McCrindle, R.; Ferguson, P. L.; Higgins, C. P.; Field, J. A. Discovery of 40 classes of per-and polyfluoroalkyl substances in historical aqueous film-forming foams (AFFFs) and AFFF-impacted groundwater. *Environ. Sci. Technol.* **2017**, *51* (4), 2047−2057.
(30) D'Agostino, L. A.; Mabury, S. A. Certain perfluoroalkyl and polyfluoroalkyl substances associated with aqueous film forming foam are widespread in Canadian surface waters. *Environ. Sci. Technol.* **2017**, *51* (23), 13603−13613.
(31) D'Agostino, L. A.; Mabury, S. A. Identification of Novel Fluorinated Surfactants in Aqueous Film Forming Foams and Commercial Surfactant Concentrates. *Environ. Sci. Technol.* **2014**, *48* (1), 121−129.
(32) Gebbink, W. A.; van Asseldonk, L.; van Leeuwen, S. P. Presence of emerging per-and polyfluoroalkyl substances (PFASs) in river and drinking water near a fluorochemical production plant in the Netherlands. *Environ. Sci. Technol.* **2017**, *51* (19), 11057−11065.
(33) Song, X.; Vestergren, R.; Shi, Y.; Huang, J.; Cai, Y. Emissions, transport, and fate of emerging per-and polyfluoroalkyl substances from one of the major fluoropolymer manufacturing facilities in China. *Environ. Sci. Technol.* **2018**, *52* (17), 9694−9703.
(34) Wang, Y.; Yu, N.; Zhu, X.; Guo, H.; Jiang, J.; Wang, X.; Shi, W.; Wu, J.; Yu, H.; Wei, S. Suspect and nontarget screening of per- and polyfluoroalkyl substances in wastewater from a fluorochemical manufacturing park. *Environ. Sci. Technol.* **2018**, *52* (19), 11007−11016.
(35) Chen, H.; Yao, Y.; Zhao, Z.; Wang, Y.; Wang, Q.; Ren, C.; Wang, B.; Sun, H.; Alder, A. C.; Kannan, K. Multimedia distribution and transfer of per- and polyfluoroalkyl substances (PFASs) surrounding two fluorochemical manufacturing facilities in Fuxin, China. *Environ. Sci. Technol.* **2018**, *52* (15), 8263−8271.
(36) Barzen-Hanson, K. A.; Field, J. A. Discovery and implications of C2 and C3 perfluoroalkyl sulfonates in aqueous film-forming foams and groundwater. *Environ. Sci. Technol. Lett.* **2015**, *2* (4), 95−99.
(37) Lang, J. R.; Allred, B. M.; Peaslee, G. F.; Field, J. A.; Barlaz, M. A. Release of per- and polyfluoroalkyl substances (PFASs) from carpet and clothing in model anaerobic landfill reactors. *Environ. Sci. Technol.* **2016**, *50* (10), 5024−5032.
(38) Niu, J.; Lin, H.; Xu, J.; Wu, H.; Li, Y. Electrochemical mineralization of perfluorocarboxylic acids (PFCAs) by Ce-doped modified porous nanocrystalline PbO_2 film electrode. *Environ. Sci. Technol.* **2012**, *46* (18), 10191−10198.
(39) Campbell, T. Y.; Vecitis, C. D.; Mader, B. T.; Hoffmann, M. R. Perfluorinated surfactant chain-length effects on sonochemical kinetics. *J. Phys. Chem. A* **2009**, *113* (36), 9834−9842.
(40) Park, H.; Vecitis, C. D.; Cheng, J.; Choi, W.; Mader, B. T.; Hoffmann, M. R. Reductive defluorination of aqueous perfluorinated alkyl surfactants: Effects of ionic headgroup and chain length. *J. Phys. Chem. A* **2009**, *113* (4), 690−696.
(41) Bao, Y.; Deng, S.; Jiang, X.; Qu, Y.; He, Y.; Liu, L.; Chai, Q.; Mumtaz, M.; Huang, J.; Cagnetta, G.; Yu, G. Degradation of PFOA substitute: GenX (HFPO−DA ammonium salt): Oxidation with UV/persulfate or reduction with UV/sulfite? *Environ. Sci. Technol.* **2018**, *52* (20), 11728−11734.
(42) Liu, J.; Van Hoomissen, D. J.; Liu, T.; Maizel, A.; Huo, X.; Fernández, S. R.; Ren, C.; Xiao, X.; Fang, Y.; Schaefer, C. E. Reductive defluorination of branched per-and polyfluoroalkyl substances with cobalt complex catalysts. *Environ. Sci. Technol. Lett.* **2018**, *5* (5), 289−294.
(43) Park, S.; de Perre, C.; Lee, L. S. Alternate reductants with VB12 to transform C8 and C6 perfluoroalkyl sulfonates: Limitations and insights into isomer-specific transformation rates, products and pathways. *Environ. Sci. Technol.* **2017**, *51* (23), 13869−13877.
(44) Wang, Z.; Wang, Y.; Li, J.; Henne, S.; Zhang, B.; Hu, J.; Zhang, J. Impacts of the degradation of 2,3,3,3-tetrafluoropropene into trifluoroacetic acid from its application in automobile air conditioners in China, the United States, and Europe. *Environ. Sci. Technol.* **2018**, *52* (5), 2819−2826.
(45) Grossweiner, L. I.; Swenson, G. W.; Zwicker, E. F. Photochemical generation of the hydrated electron. *Science* **1963**, *141* (3583), 805−806.
(46) Fischer, M.; Warneck, P. Photodecomposition and photooxidation of hydrogen sulfite in aqueous solution. *J. Phys. Chem.* **1996**, *100* (37), 15111−15117.
(47) Song, Z.; Tang, H.; Wang, N.; Zhu, L. Reductive defluorination of perfluorooctanoic acid by hydrated electrons in a sulfite-mediated UV photochemical system. *J. Hazard. Mater.* **2013**, *262*, 332−338.
(48) Tian, H.; Gao, J.; Li, H.; Boyd, S. A.; Gu, C. Complete defluorination of perfluorinated compounds by hydrated electrons generated from 3-indole-acetic-acid in organomodified montmorillonite. *Sci. Rep.* **2016**, *6*, 32949.
(49) Sun, Z.; Zhang, C.; Xing, L.; Zhou, Q.; Dong, W.; Hoffmann, M. R. UV/nitrilotriacetic acid process as a novel strategy for efficient photoreductive degradation of perfluorooctanesulfonate. *Environ. Sci. Technol.* **2018**, *52* (5), 2953−2962.
(50) Gu, Y.; Dong, W.; Luo, C.; Liu, T. Efficient reductive decomposition of perfluorooctanesulfonate in a high photon flux UV/sulfite system. *Environ. Sci. Technol.* **2016**, *50* (19), 10554−10561.
(51) Gu, Y.; Liu, T.; Wang, H.; Han, H.; Dong, W. Hydrated electron based decomposition of perfluorooctane sulfonate (PFOS) in the VUV/sulfite system. *Sci. Total Environ.* **2017**, *607*, 541−548.
(52) Gu, Y.; Liu, T.; Zhang, Q.; Dong, W. Efficient decomposition of perfluorooctanoic acid by a high photon flux UV/sulfite process: Kinetics and associated toxicity. *Chem. Eng. J.* **2017**, *326*, 1125−1133.
(53) Banks, R. E.; Smart, B. E.; Tatlow, J. *Organofluorine Chemistry: Principles and Commercial Applications*; Springer Science & Business Media, 2013.
(54) Paul, A.; Wannere, C. S.; Schaefer, H. F. Do linear-chain perfluoroalkanes bind an electron? *J. Phys. Chem. A* **2004**, *108* (43), 9428−9434.

DOI: 10.1021/acs.est.8b06648
Environ. Sci. Technol. 2019, 53, 3718−3728

(55) Nohara, K.; Toma, M.; Kutsuna, S.; Takeuchi, K.; Ibusuki, T. Cl atom-initiated oxidation of three homologous methyl perfluoroalkyl ethers. *Environ. Sci. Technol.* **2001**, *35* (1), 114−120.
(56) Hori, H.; Hayakawa, E.; Einaga, H.; Kutsuna, S.; Koike, K.; Ibusuki, T.; Kiatagawa, H.; Arakawa, R. Decomposition of environmentally persistent perfluorooctanoic acid in water by photochemical approaches. *Environ. Sci. Technol.* **2004**, *38* (22), 6118−6124.
(57) Vandamme, M.; Bouchard, L.; Gilbert, A.; Keita, M.; Paquin, J.-F. Direct esterification of carboxylic acids with perfluorinated alcohols mediated by XtalFluor-E. *Org. Lett.* **2016**, *18* (24), 6468−6471.
(58) Yuan, G.; Peng, H.; Huang, C.; Hu, J. Ubiquitous occurrence of fluorotelomer alcohols in eco-friendly paper-made food-contact materials and their implication for human exposure. *Environ. Sci. Technol.* **2016**, *50* (2), 942−950.
(59) Suenram, R.; Lovas, F.; Pickett, H. Fluoromethanol: Synthesis, microwave spectrum, and dipole moment. *J. Mol. Spectrosc.* **1986**, *119* (2), 446−455.
(60) Qu, Y.; Zhang, C.; Li, F.; Chen, J.; Zhou, Q. Photo-reductive defluorination of perfluorooctanoic acid in water. *Water Res.* **2010**, *44* (9), 2939−2947.
(61) Houtz, E. F.; Sedlak, D. L. Oxidative conversion as a means of detecting precursors to perfluoroalkyl acids in urban runoff. *Environ. Sci. Technol.* **2012**, *46* (17), 9342−9349.
(62) Harding-Marjanovic, K. C.; Houtz, E. F.; Yi, S.; Field, J. A.; Sedlak, D. L.; Alvarez-Cohen, L. Aerobic biotransformation of fluorotelomer thioether amido sulfonate (Lodyne) in AFFF-amended microcosms. *Environ. Sci. Technol.* **2015**, *49* (13), 7666−7674.
(63) Tian, H.; Gu, C. Effects of different factors on photo-defluorination of perfluorinated compounds by hydrated electrons in organo-montmorillonite system. *Chemosphere* **2018**, *191*, 280−287.

DOI: 10.1021/acs.est.8b06648
Environ. Sci. Technol. 2019, 53, 3718−3728